AFGC-ACI-*fib*-RILEM Int. Symposium on Ultra-High Performance Fibre-Reinforced Concrete,
UHPFRC 2017 – October 2-4, 2017, Montpellier, France

FINITE ELEMENT ANALYSIS ON PULL-OUT BEHAVIOR OF POST-INSTALLED ADHESIVE ANCHOR FILLED WITH UHPFRC

Ayumi Satoh (1), Yuki Sakagami (1) and Shun Mitarai (1)

(1) Kumamoto University, Kumamoto, Japan

Abstract

Experimental pull-out test and finite element analysis (FEM) are conducted in order to discuss the pull-out behaviour of post-installed adhesive anchor filled with ultra-high performance fibre reinforced concrete (UHPFRC) as an adhesive. The numerical results by the FEM revealed that the constitutive laws of interface elements between the substrate concrete and the adhesive significantly affect the peak load and the deformation of post-installed adhesive anchor under the pull-out force. It suggests the significance of the mechanical properties of the interface, i.e., the surface treatment of the hole for the anchor in the substrate concrete. Furthermore, analytical results were consistent to the experimental crack pattern of mixed bond-cone failure of the adhesive anchor. The development process of the crack pattern is also analysed step by step, which shows a mechanism derived from the uniform development of shear stress along the depth of the anchor due to the high modulus of the adhesive UHPFRC.

Résumé

Des essais d'arrachement et leur analyse aux éléments finis ont été réalisés afin d'analyser le comportement à l'arrachement d'ancrages adhérents rapportés scellés avec du béton fibré à ultra-hautes performances (BFUP). Les résultats de l'analyse aux éléments finis ont révélé que les lois de comportement des éléments d'interface entre le support béton et l'adhésif affectent de manière significative la charge maximale et la déformation de l'ancrage adhérent rapporté avant d'atteindre la force d'extraction. D'où l'importance des propriétés mécaniques de l'interface, c'est-à-dire le traitement de surface de la réservation pour ancrage dans le substrat en béton. En outre, les résultats analytiques se sont révélés cohérents avec le facies de fissuration expérimental, avec une rupture mixte glissement / rupture en cône de l'ancrage. Le processus de fissuration a également été analysé pas à pas, mettant en évidence un mécanisme dérivé du développement uniforme de la contrainte de cisaillement le long de la profondeur de l'ancrage, en raison du module élevé du BFUP réalisant le scellement.

1. INTRODUCTION

The post-installed adhesive anchor is very convenient for repairing concrete structures and attaching some peripherals to concrete substrate [1-3]. However, because the adhesive for the anchor is mainly made of resin, the degradation of the adhesive is feared and actually had caused a well-known fatal accident in Japan. On the other hand, cementitious materials have the excellent durability and the fire resistance capability compared with resin. Among the cementitious material, Ultra-High Performance Fibre-Reinforced Concrete (UHPFRC) has the outstanding durability. The authors have been conducting research experimentally and analytically with the aim to develop a new type of adhesive made of cement-based material, which is the main target of this study. In this study, experimental pull-out test and finite element analysis are conducted in order to discuss the pull-out behaviour of post-installed adhesive anchor bonded with UHPFRC as an adhesive.

2. EXPERIMENT AND RESULTS

2.1 Specimens and materials used

We conducted pull-out tests to investigate the pull-out behaviour of the post-installed adhesive anchor filled with UHPFRC. As shown in Figure 1, the test specimens consist of a cylindrical concrete blocks with dimensions of 300mm (in diameter) × 150mm (in depth) in which the anchor bolts were embedded. The drilled holes in concrete blocks measure 30mm in diameter (as a fixed condition), and 25, 50 and 75 mm in lengths (as variable conditions). UHPFRC was used as the anchoring adhesive. The specimens are named to identify their diameter of the drilled hole and the embedment depth as given in Table 1. Two test specimens are prepared for each condition and are denoted as No. 1 and No. 2, respectively in Table 1. The concrete blocks were cast using ready-mixed concrete Grade 40-N-18-20-N (in JIS standard). The composition of the UHPFRC for the anchoring adhesive and the mix proportion of UHPFRC are listed in Table 2 and Table 3, respectively.

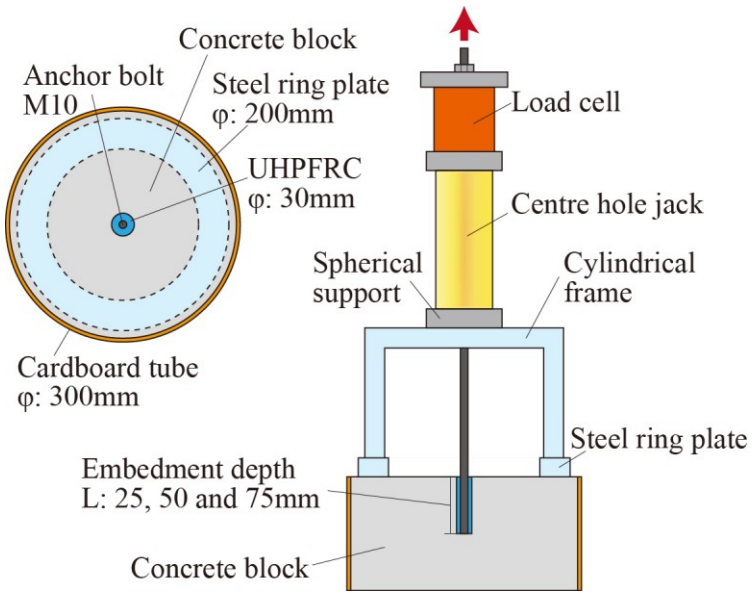

Figure 1: Detail of specimen and experimental set-up

The anchor bolts used in this study were SNB7 threaded rods with tensile strengths of 822 MPa (in yield tress) and 1033 MPa (in ultimate stress) which nominally measure 9.025 mm in diameter (M10 bolts in JIS). Mechanical properties of concrete and UHPFRC are given in Table 4. Compressive strength and tensile strength of UHPFRC were determined using cylindrical specimens measured 50 mm (in diameter) × 100 mm (in height).

Concrete blocks were cured with wet clothes for 7 days and drilled with a hammer drill at the age of 14 days. At the drilling, concrete dust around the drilled hole was vacuumed perfectly. The anchor bolts were fixed with using UHPFRC adhesive to the expected locations slowly to obtain air free bond. The UHPFRC was mixed in an Omni-mixer, the batch size of which measures 5 litters. Any heat or pressure treatments were not applied during casting or curing, reflecting the real construction conditions. The specimens were stored in room condition for 14 days.

Figure 1 shows the test set-up used for the pull-out test. A cylindrical frame was used as a support of a centre hole jack to pull-out the anchor bolts from concrete blocks. Axial load was applied to the specimens with low increments up to maximum load. The inner diameter of the steel ring plate was 200 mm, which we considered to have the enough space to avoid the confined force around the anchor bolt. The pull-out deformation of anchor bolt was measured using displacement transducer attached at the height of 50 mm from the upper surface of the concrete block.

Table 1: Charachteristics of test speciemns and test results

Specimen	No.	Diameter of drilled hole (mm)	embedment depth (mm)	Maximum Load (kN)	Failure* mode
U-D30-L25	1	30.0	25.0	15.1	B
	2			16.5	C
U-D30-L50	1	30.0	50.0	37.1	B
	2			39.7	D
U-D30-L75	1	30.0	75.0	51.1	D
	2			51.9	D

*B: Bond failure, C: Concrete cone failure, D: Mixed bond-cone failure

Table 2: Materials used in this study

	Detail of materials	
Binder	Low-heat portland cement (C) Density: 3.21 g/cm^3	Silica fume (SF) Density: 2.20 g/cm^3
	Blast-furnace slag (BFS) Density: 2.89 g/cm^3 Specific surface: 6,000 cm^2/g	Dehydrate gypsum (Gy) Density: 2.23 g/cm^3
Aggregate	Silica sand No.8 (Sand 8) Density: 2.50 g/cm^3	Silica sand No.6 (Sand 6) Density: 2.59 g/cm^3
Admixture	Superplasticizer (Ad), Polycarboxylic acid type	
Fiber	Straight type steel fiber (fiber), Size: Diameter 0.16 mm × Length 6 mm Tensile strength: 2,000 N/mm^2	

2.2 Test results

Figure 2 shows the measured load-displacement curves of specimens obtained from the pull-out test. The maximum load and failure modes of the pull-out tests are summarized in Table 1. As seen Table 1 and Figure 2, the maximum load significantly increased with the increasing embedment depth of the anchor bolts.

In this study, typical failure modes of adhesive anchor bolt under pull-out loading are classified into 4 types of failure: anchor bolt failure, bond failure, concrete cone failure and mixed bond-cone failure. Among them, a schematic diagram of mixed bond-cone failure is shown in Figure 3. Figure 3 represents a crack pattern of the specimen (U-D30-L75 No.2) cut in the centre of the specimen after the pull-out test. It shows the cone failure in the substrate concrete, which caused the anchor bolt to pull-out from the concrete block. Table 1 shows that the failure mode gradually changed from the bond failure to mixed bond-cone failure according to the increase of the embedment depth of the anchor bolt.

Table 3: Mix proportion of UHPFRC

W/B (%)	Unit weight (kg/m^3)								
	W	C	SF	BFS	Gy	Sand 8	Sand 6	Ad	Fiber
20	177	600	67	432	83	187	748	59	157

* W/B: Water-Binder ratio, W: Water

Table 4: Mechanical properties of concrete and UHPFRC

	Compressive strength (N/mm^2)	Young's modulus (kN/mm^2)	Tensile Strength (N/mm^2)	Flexural strength (N/mm^2)
Concrete	50.3	31.0	3.36	-
UHPFRC	99.8	35.0	9.89	24.1

*Concrete: Standard curing for 28 days
*UHPFRC: Job-site curing for 14 days

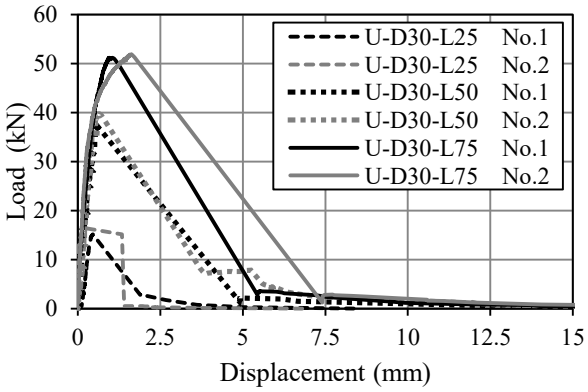

Figure 2: Experimental load-displacement curves

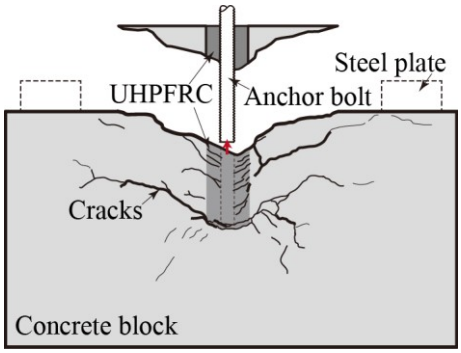

The bond failure develops in the depth along the anchor bolt accompanied with the cone failure of concrete in the shallow part of the embedment.

Figure 3: Crack pattern of mixed bond-cone failure (U-D30-L75 No.2)

3. FINITE ELEMENT ANALYSIS

3.1 Detail of analysis

A multi-purpose structural analysis FEM program was employed for solving the models. In this study, specimen U-D30-L75 were modeled. FEM models in Figure 4 are 2-dimensional axisymmetric model reflecting the symmetry of cylindrical specimens which consist of quadrilateral elements sized 2.5 mm × 2.5 mm. We applied a four-node isoparametric axisymmetric solid ring element with a quadrilateral cross-section. Two dimensional interface elements were placed between concrete elements and UHPFRC ones. As shown in Table 5, we analyzed 7 cases of the model in which the material constitutive laws of interface elements were changed. They are described below in section 3.2.

Figure 4 tells that the left edges are horizontally fixed and vertically free, and also that the upper edges of steel plate are vertically fixed and horizontally free. The edge of the anchor bolt, where the arrow is drawn, moved in the upper direction at a step of 0.02 mm in the non-linear analysis. The plane stress condition was applied to all the elements for which the dispersed crack characteristics were applied. Rotated crack model was assumed after cracking. The step of non-linear analysis based on the increase of deformation, which is controlled with the energy-based norm. When solving the model, the iteration of each step followed the Newton-Raphson method.

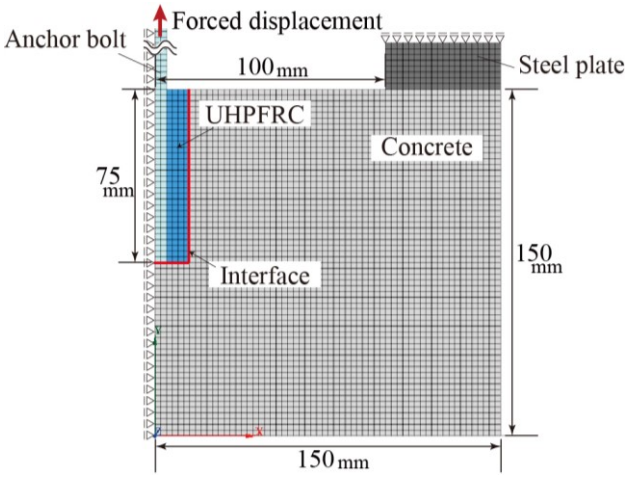

Figure 4: Finite element mesh

Table 5: Analysis models

Model	Interface element		
	Shear bond stress (N/mm^2)	Shear stiffness K (N/mm^3)	Shear bond softening of Shear stress – relative displacement curve
B	10.0	60.0	Brittle
P			Perfect elastoplasticity
S5			Softening modulus: 1/5 of K
S10			Softening modulus: 1/10 of K
S25			Softening modulus: 1/25 of K
S50			Softening modulus: 1/50 of K
S100			Softening modulus: 1/100 of K

3.2 Material constitutive law

Figure 5(a) represents the material constitutive laws applied to the elements of concrete. The compressive stress-strain curve of concrete is the one obtained by the Popovics' equation (1).

$$\sigma = F_c \frac{n(\varepsilon/\varepsilon_{co})}{n-1+(\varepsilon/\varepsilon_{co})^n} \quad (1)$$

Where E is compressive stress (N/mm^2); ε is compressive strain; Fc is compressive strength (N/mm^2); ε_{co} is strain at compressive strength; and n is empirical constant. The test results shown in Table 4 were used for the compressive strength (Fc) and Young's modulus of concrete (Ec).

In the right graph of Figure 5(a), the constitutive law on the tension side of the concrete is made with the tensile strength (Ft) and the Hordijk's softening curve [4]. In the graph, h is the equivalent length of the element, and GF (0.1 N/mm) is the fracture energy of concrete.

Figure 5(b) represents the material constitutive laws applied to the elements of UHPFRC. The compressive strength and Young's modulus given in Table 4 were used for them. The compressive stress-strain curve of UHPFRC is modelled after a linear elasticity until the compressive strength and a uniform softening inclination after that. The tensile stress-strain curve shown in Figure 5 (b) was determined by the uniaxial tensile test with dumbbell specimen [5].

The material constitutive law adopted for anchor bolt is based on von Mises yield criterion, shown in Figure 5(c). In the graph, Es means Young's modulus of anchor bolt and H' is strain hardening index set at Es/1000.

Constitutive behaviour of the interface elements is described in two terms of relationships across the interface: the one between normal stress and normal relative displacement, and the one between shear effective stress and shear relative displacement. Figure 6 (a) shows the stress-relative displacement curve in the normal direction of the interface element, where the debonding is considered. Seven types of the stress-relative displacement curves in the shear direction were analysed as shown in Figure 6 (b). Except for the different softening behaviour of all 7 models, shear bond strength and shear stiffness (K) were fixed to 60.0 (N/mm^3) and 10.0 (N/mm^2) respectively. Seven types of the softening properties (referred to shear bond softening in this paper) after reaching the shear bond strength were studied parametrically. As shown in Figure 6, Model B is completely brittle and model P is perfect elasto-plastic, whereas other 5 models (from S5 to S100) are made to have the different softening behaviour at the gradient from 1/5 to 1/100 of the shear stiffness. Among them, model S5 or S10 are similar to the property that agree with the well-known "shear lag theory".

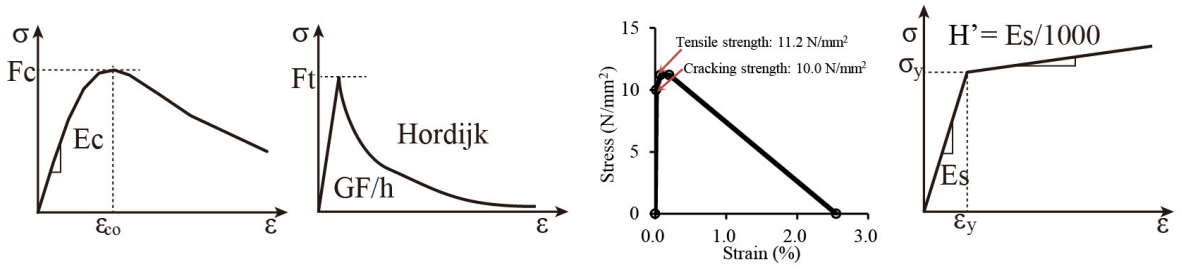

(a) Concrete (b) UHPFRC (c) Anchor bolt

Figure 5: Constitutive models of materials

4. ANALYSIS RESULTS AND DISCUSSION

4.1 Load-displacement curves

The resulted load-displacement curves of the post-installed adhesive anchor calculated by finite element analysis are depicted in Figure 7. The displacement curves in Figure 7 are obtained from the movement of the node of the anchor bolt at 50 mm high from the upper surface of the concrete, where the experimental measurement was conducted. In Figure 7, the load-displacement curves of the analysed ones can be compared with the experimental ones. It is shown that the load-displacement curves of the model S10 and S25 are consistent to the experimental results. The pull-out softening behaviours are more clearly affected by the shear bond softening parameter than the peak loads. In this analysed results, the ductility in the pull-out behaviour increased as the gradient of the shear bond softening property becomes gentle.

4.2 Development process of crack pattern

Figure8 illustrates the crack patterns of the experimental result and the analysed one of model S10. The crack pattern of the analysed result is depicted under a condition that the analysed strain in the x direction is larger than the strain which corresponds to 0.05 mm in the crack width. The analysed crack pattern matched well the experimental results, as seen in Figure 8.

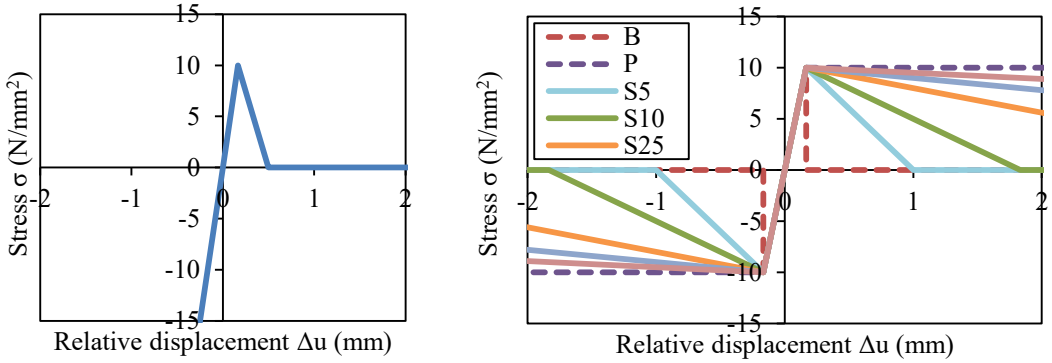

(a) Model for normal stress (b) Models for shear stress

Figure 6: Constitutive models for interface element

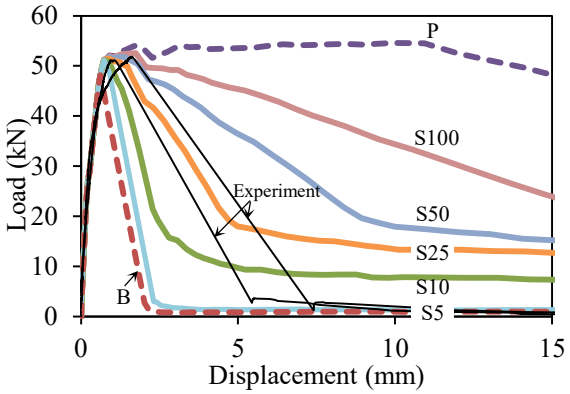

Figure 7: Analytical result of load-displacement curves

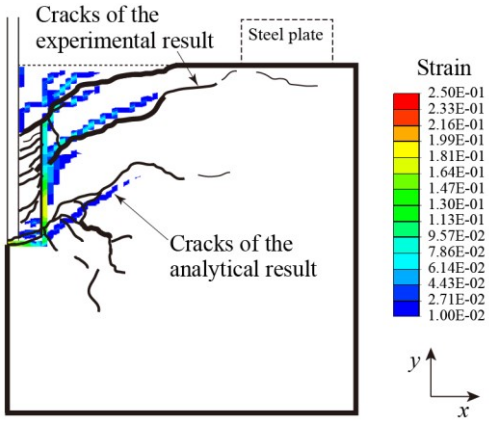

Figure 8: Comparison between experimental crack pattern and analytical one (model S10 at peak load)

Figure 9(a) to 9(d) describe the process of crack pattern propagation with the shear adhesive stress distribution at each load step of the model S10. The crack patterns of the analysed result in Figure 9 are visualized with narrower cracks than 0.05mm (i.e., micro cracks). As seen in Figure 9(a), micro cracks occurred in the concrete near the interface between concrete and UHPFRC, and then a primary crack appears with forming the cone failure in substrate concrete. At that state, the shear adhesive stress distribution is almost uniform along the depth of embedded anchor bolt. Though stress model follows the "shear lag theory"[6], this result is not consistent to the theory which predict the maximum shear stress at the top and exponentially decreasing shear stress along the depth. This special stress distribution derives from two causes: one is the high rigidity of the adhesive UHPFRC, and another is the accumulating micro and primary cracks in upper part of concrete which make the shear stress transfer ineffective at the upper part, eventually making the bottom part highly effective.

In Figure 9(b) and 9(c), the second and third cracks expand at the middle and the deepest position of the embedment respectively. At the same time, the crack width near the interface between concrete and UHPFRC has grown. From the shear stress distribution in the same figures, it is seen that the above mentioned cracks make the stress distribution uneven yielding higher shear stress at the deeper depth. In Figure 9(c) which represents the results of the peak load, the region in which the stress excels the shear strength (10.0 N/mm^2) expands along the depth.

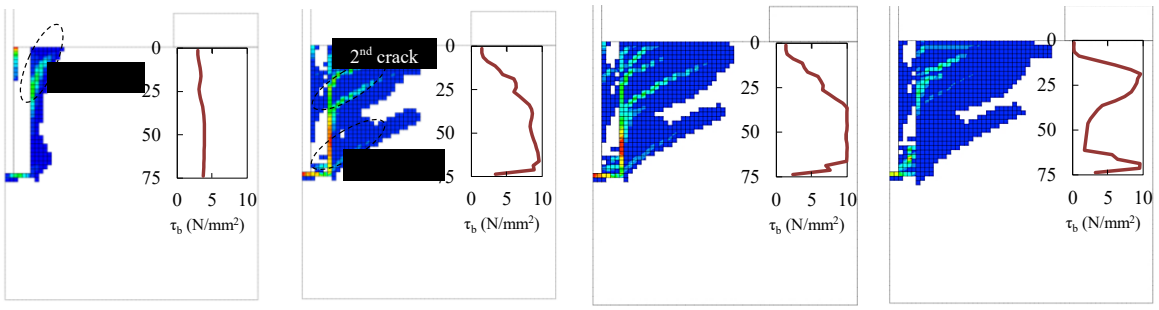

(a) P=27.3kN (b) P=48.1kN (c) P=51.2kN (Peak load) (d) P=33.4kN

Figure 9: Crack pattern propagation and shear bond stress distribution of model S10

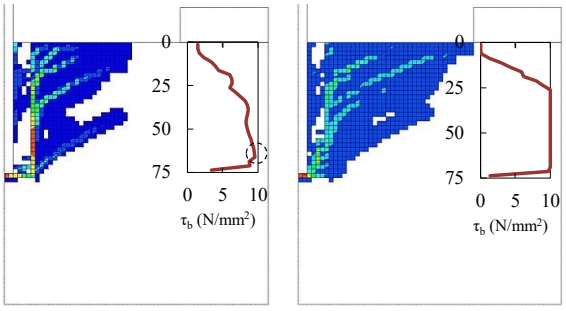

(a) Model B(P=48.1kN) (b) Model P(P=54.0kN)

Figure 10: Analytical crack patterns and shear bond stress distribution at peak load

The crack pattern in Figure 9(d), which represents the results of softening state, shows the mixed bond-cone failure that corresponds to the experimental result. This failure mode derives from both the localization process to the first crack and the loss of the bond at about 50 mm in depth. At that state, shear stress of the interface at about 50 mm in depth decreases and the pull-out load decreases accordingly.

4.3 Difference of crack patterns

Figure 10(a) and 10(b) represent the crack patterns with the shear stress distribution graphs of model B and model P. Figure 10(a) shows the results of model B which showed the brittle failure in Figure 7. The brittle failure is caused after the peak load when the interface elements (marked in dotted line in Figure 10) reached the shear strength (10.0 N/mm2). Figure 10(b) shows the results of model P, where it is shown that the cone-shaped crack propagates from the bottom aslant along with the extension of the micro crack region. The mechanism behind it is caused from the ductile property of the interface, which brings the small ineffective region that yields low shear stress at the top and the large effective region that bears maximum shear stress (shear strength) at the deeper region. The peak load occurs at the moment when the low stress region reached at 25mm in depth and the remaining region (50 mm in length) holds the maximum shear stress. The crack pattern, the stress distribution at the maximum load of model S10 (in Figure 9(c)) are the averaged ones of the model B and model P shown in Figure 10(a) and 10(b).

Thus, the analytical load-displacement curves and the crack patterns are consistent to the experimental results when the analytical models include the adequate interface properties between substrate concrete and UHPFRC adhesive. It is suggested that the gentle softening gradient of the shear stress yields the enhanced maximum pull-out load and the ductile failure mode of the post-installed adhesive anchor.

5. CONCLUSION

In this study, experimental pull-out test and finite element analysis were conducted in order to discuss the pull-out behaviour of post-installed adhesive anchor bonded with UHPFRC. FEM analysis suggested the clues for further enhancing the performance of the pull-out behaviour of post-installed adhesive anchor. The findings are as follows.

(1) Several inner cracks were also found at the section of the sawn specimen after the pull-out test except for the cracks from the cone failure.

(2) The high rigidity of the adhesive UHPFRC and the accumulating micro and primary cracks in upper part of concrete make the shear stress transfer ineffective at the upper part, eventually making the bottom part highly effective.

(3) The analytical load-displacement curves and the crack patterns are consistent to the experimental results when the analytical models include the adequate interface properties between substrate concrete and UHPFRC adhesive.

(4) It is suggested that the gentle softening gradient of the shear stress in the interface element of the model yields the enhanced maximum pull-out load and the ductile failure mode of the post-installed adhesive anchor.

ACKNOWLEDGEMENTS

This work was supported by JSPS KAKENHI Grant Number JP16K18189. The author also would like to thank Professor Kiyoshi Murakami, Associate professor Koji Takeda and technical staff Yoshinori Toda at Kumamoto University, and Professor emeritus Kanji Yamada at Akita prefectural University for their contributions to the project.

REFERENCES

[1] Epackachi, S. et al., 'Behavior of adhesive bonded anchors under tension and shear loads', Journal of Constructional Steel Research. **114** (2015) 269-280.
[2] Yilmaz, S. et al., 'Tensile behavior of post-installed chemical anchors embedded to low strength concrete', Construction and Building Materials. **47** (2013) 861-866.
[3] Kim, J-S. et al., 'Performance evaluation of the post-installed anchor for sign structure in South Korea', Construction and Building Materials. **44** (2013) 496-506.
[4] Hordijk, D. A.: Local Approach to Fatigue of Concrete, PhD thesis, Delft University of Technology (1991)
[5] Satoh, A et al., 'Flexural Behavior of RC Beams with UHPFRC Permanent Form', Proceedings of the Japan Concrete Institute. **38**(1) (2016) 2361-2366.
[6] Greszczuk, L B., 'Theoretical Studies of the Mechanics of the Fiber-Matrix Interface in Composites', In Interfaces in Composites, American Society of Testing and Materials, ASTM STP 452, Philadelphia (1969) 452-58.